Adaptability and accuracy of all-electron pseudopotentials

Jiří Vackář and Antonín Šimůnek
Institute of Physics, Academy of Sciences of the Czech Republic, Cukrovarnická 10, 162 53 Praha 6, Czech Republic
(Received 19 August 2002; revised manuscript received 22 November 2002; published 19 March 2003)

We suggest several ways of improving pseudopotential transferability within the approach based on all-electron self-consistent pseudopotentials. Particularly, we show that the pseudopotentials constructed for two energy channels and using the pseudized core charge included in exchange and correlation potential terms, can provide an exact and stable solution for cases where the current pseudopotential methods encounter difficulties and need special treatment. Examples such as semicore states participating in the chemical bond, extended valence states, or a significant charge transfer in alkali chlorides are presented. The need for the semiempirical choice of ''suitable'' atomic configuration in the pseudopotential generating process is eliminated and also the higher *l*-pseudopotential components are generated in a natural way. Also some general aspects of pseudopotential transferability are discussed in detail.

DOI: 10.1103/PhysRevB.67.125113 PACS number(s): 71.10.−w, 71.15.−m

I. INTRODUCTION

The *ab initio* density-functional approach has proven to be a reliable and accurate tool for the electronic state calculation in solids over several decades, being applied in a large variety of diverse areas. The only approximation required in applying density-functional theory (DFT) for practical calculations is, in principal, some model for the exchange and correlation potential, since the functional of the charge density describing the exchange and correlation effects is not known generally. Additional approximations, however, are specific for various computational methods, consisting of a particular choice of a basis set and/or shape approximations to the potential in selected regions.

First-principles pseudopotential techniques, as reviewed by Pickett[1] and Payne *et al.*,[2] provide an efficient linearized tool for separating core and valence electron interactions, in principle, mathematically accurate to the first order within the chosen approximation to DFT. Several various pseudopotential construction techniques, having been introduced during the past decades, approach this ideal more or less, each of them having its own approximations, drawbacks, computational difficulties, and artificial ''technical'' parameters impairing their *ab initio* character.

In this paper we discuss the flaws of standard pseudopotential techniques being used at present and we investigate the potential sources of errors and inaccuracies. Particularly, we deal with the concept of pseudopotential transferability and we suggest several approaches to reducing the transferability-related errors within the all-electron pseudopotential (AEPP) method.[3]

In the next two sections, we give a brief exposition of AEPP construction, stressing the differences of the standard approaches and significant points with respect to pseudopotential transferability. The third section deals with the concept of pseudopotential transferability generally, analyzes the flaws of standard techniques in this respect, and then summarizes the merits of the AEPP method. The fourth section illustrates the advantages of the present technique with particular materials, where standard pseudopotentials usually meet difficulties and/or need special treatment.

II. ALL-ELECTRON PSEUDOPOTENTIAL METHOD

By standard conditions that pseudopotentials satisfy, by definition, i.e., the conditions for the values and derivatives of relevant quantities at the cutoff radius R_C, the shape of the pseudopotential is not determined completely. In fact, there is an infinite number of ways of creating the pseudopotential inside the core region of an atom. By a particular pseudopotential technique, redundant degrees of freedom can be used for optimizing the pseudopotential in various respects in order that the pseudopotential has suitable properties. In this section we describe a method that uses this freedom in a particular way, that we describe in the next paragraphs.

In some cases the spatial range of the core states (states of the fully occupied atomic shells) significantly extends beyond the core region of an atom in the usual sense. These states, denoted as semicore states, can be included in the valence basis by constructing ''conservative'' pseudopotentials for these states [for example, $3s$ and $3p$ states of Mn (Ref. 4) or of K] with no respect to the valence states. The resulting pseudopotentials then describe valence electrons with undefined accuracy by means of excited pseudofunctions, i.e. pseudofunctions with a node.

The AEPP technique constructs pseudopotentials consistent with the valence electron charge density in a solid. If one can suppose that the semicore states are significant in a particular case, the AEPP's for the valence states can be generated so that the corresponding pseudowave functions related to the valence states have nodes. The redundant degrees of freedom are then used for optimizing the pseudopotentials so that the lowest-energy nodeless eigenfunctions simulate the semicore states. This ''reverse'' approach compared to the conservative pseudopotentials has several significant advantages:

(i) The AEPP is self-consistent with the valence electrons in charge distribution and angular momentum character. Additionally, the energy window of the AEPP is optimized.

(ii) Since the semicore states always correspond to a closed shell of an atom, their pseudofunctions can be renor-

malized to get softer, smooth, and computationally more convenient pseudopotentials.

(iii) The effects of the semicore states can be included (by iterations) into simple pseudopotentials with nodeless pseudofunctions for valence electrons. This produces a soft pseudopotential, eliminates the frozen-core approximation, decreases the size of a plane-wave basis set, and it can be useful for band-structure calculations in a dense k mesh in the Brillouin zone.

The AEPP is described in detail in Ref. 3. Here we present the equations necessary for understanding the essential features of the AEPP technique.

The initial step of an all-electron-pseudopotential-generating procedure provides an all-electron atomic calculation where the valence states are treated self-consistently with the calculation in a solid. The charge density corresponding to valence radial atomic wave functions $R_{E,l}(r)$ matches the partial charge density in a solid by the logarithmic derivative at the cutoff radius R_C,

$$\frac{d}{dr}\ln[r^2|R^{\mathrm{at}}_{E_{\mathrm{val},l},l}(r)|^2]\Big|_{r=R_C}=\frac{d}{dr}\ln[r^2\rho_l^{\mathrm{sps}}(r)]\Big|_{r=R_C}, \quad (1)$$

where the partial charge density in a solid $\rho_l^{\mathrm{sps}}(r)$ is evaluated by summing over all occupied states,

$$\rho_l^{\mathrm{sps}}(r)=\sum_{\vec{k},n}\sum_{m=-l}^{l}\frac{1}{4\pi r^2}\int_{SPH}d\Omega\, d\Omega'\,\psi^*_{\vec{k},n} \times(r\hat{\mathbf{n}})Y_{lm}(\hat{\mathbf{n}})Y^*_{lm}(\hat{\mathbf{n}}')\psi_{\vec{k},n}(r\hat{\mathbf{n}}'), \quad (2)$$

where $\psi_{\vec{k},n}$ denotes the crystal pseudowave function with $\vec{k}$ as the vector of the first Brillouin zone and a band index n.

The boundary condition of Eq. (1) replaces the standard condition for the wave functions to be normalizable and determines the eigenvalue E_l. The normalization condition for the valence atomiclike radial wave functions is

$$\int_0^{R_C}|R^{\mathrm{at}}_{E_{\mathrm{val},l},l}(r)|^2r^2dr=\int_0^{R_C}\rho_l^{\mathrm{sps}}(r)r^2dr. \quad (3)$$

Using the results of the self-consistent atomiclike calculation with the boundary conditions of the solid, we apply the phase-shift technique[5] for the construction of pseudopotentials. By varying the screened pseudopotential, this technique minimizes a functional assembled from a set of conditions to be satisfied by the pseudopotential. The common condition requiring the continuous augmentation of the pseudowave function at the cutoff radius R_C is transformed into a condition for the generalized phase shift that depends on the energy monotonously, which ensures the numerical stability and gives the name to the technique.

Each component $V_l^{\mathrm{scr}}(r)$ of the screened pseudopotential is constructed in such a way that the following conditions for $V_l^{\mathrm{scr}}(r)$ and for each corresponding pair of pseudowave functions (in the case of two energy windows) are fulfilled.

(i) At $r=R_C$ the potential $V_l^{\mathrm{scr}}(r)$ matches the all-electron potential $V^{\mathrm{at}}(r)$ up to the second derivative, (ii) at $r=R_C$ the radial pseudowave functions $R^{\mathrm{ps}}_{E_{n,l},l}(r)$ match the corresponding atomiclike radial functions by their values and first derivatives, and (iii) the correct energy derivative of the pseudowave function is ensured by the norm-conserving condition.

In order to avoid too hard pseudopotentials, we apply condition (iii) to the valence state only. Since the semicore states can be easily distinguished from the valence ones (by energy position, dispersion, localization, and angular momentum character) they can be simply renormalized. This represents considerable simplifications in the code compared to the ultrasoft pseudopotentials. The relaxed normalization of semicore states creates additional freedom for constructing pseudopotentials that can be employed to satisfy other conditions, e.g., those concerning optimum smoothness.

III. THE CONCEPT OF PSEUDOPOTENTIAL TRANSFERABILITY AND MERITS OF THE AEPP TECHNIQUE

In this section, before we discuss the merits of the present approach, we reflect on the concept of pseudopotential transferability generally and analyze the flaws of standard techniques in this respect. At the end of this section we summarize in which respect the AEPP technique can improve the accuracy of the pseudopotential method.

All standard pseudopotentials are derived from all-electron calculations performed for a suitable reference state of a free atom. For this reference state (used for its construction), the pseudopotential is exact. The capability of the pseudopotential to reproduce the all-electron results correctly under different environmental conditions, e.g., when the electronic configuration changes from the free atom to the atom in a particular solid, is denoted as *pseudopotential transferability*.

In fact, this term comprises two components (mutually dependent to some extent, as we will note in following paragraphs): (i) the precision of reproducing the scattering properties of the all-electron potential (represented by the logarithmic derivative of the wave function at a given radius) as a function of wave-function energy in some neighborhood of pseudopotential reference energy, and (ii) the precision of reproducing the all-electron atomic eigenvalues under changing external environmental conditions which reflect various types of chemical bonding, i.e., various neighboring atoms and various geometry. Within DFT, the external environmental conditions can be unambiguously determined by the external charge density.

The norm-conserving condition for the pseudowave function having been introduced into the pseudopotential method by Hamann[6] represented an important qualitative step in the development of the method, regardless of being partially replaced by other means within the concept of ultrasoft pseudopotentials at present.[7] As proved by Topp and Hopfield,[8] satisfying this condition ensures the correct first energy derivative of the logarithmic derivative of the pseudowave function at a certain atomic radius—exactly for the same radius for which the norm-conserving condition has been satisfied. In this sense, the pseudopotential theory is

linearized with respect to energy-level shifts. It has been shown by Shirley *et al.*[9] that the higher-order errors of pseudopotential scattering properties depend on ''higher momenta'' of the norm-conserving condition, obtained as a multiple integral of the radial charge density inside the sphere of a given radius.

Taking into account the facts mentioned above, we can see that the basic standard (first-order) norm-conserving condition ensures the correct response of the pseudowave function to the *integral* (over the given sphere) external charge density, not to varying the charge distribution inside the sphere. From another point of view—since the shift of the wave function's energy is equivalent to the same (but for the opposite sign) shift of the potential as a whole—the correct first energy derivative of scattering properties, ensured by the first-order norm-conserving condition, is equivalent to the correct pseudopotential behavior (to the first order) with respect to adding an external charge density causing a constant (inside the given sphere) potential shift. The difference between this ''ideal'' external charge density (i.e., that satisfying the condition of constant potential shift inside of the sphere) and real external charge density is a source of the first-order error, introduced above as a transferability error of type (ii).

Another source of first-order errors arises in the second step of pseudopotential construction where the screening potential terms (the Hartree and the nonlinear exchange-correlation terms) are subtracted to obtain the unscreened ionic pseudopotential, since the charge density used for unscreening can be quite different from that used for rescreening in the solid-state calculation. However, this error can be simply avoided to some extent by the *nonlinear core correction* (NLCC) which adds—and subtracts later—the approximated core charge in order to increase transferability of the nonlinear exchange and correlation terms. The NLCC was first introduced into pseudopotential calculation by Louie *et al.*,[10] and its importance for density-functional-based pseudopotential calculation was investigated recently by Porezag *et al.*[4] By means of the NLCC, the first-order error is eliminated on the condition that the used core charge density reflects the actual core charge density precisely. In practice, the core charge density is pseudized in order to avoid long plane-wave expansion or, in many cases, it is even replaced by some suitable simple analytic function of barely a similar shape.

So far, in reducing the pseudopotential method errors, effort has been made, particularly, to improve the first-order pseudopotential transferability, which led to development of various pseudopotential-constructing techniques and introducing the NLCC. Minor attention has been paid to reducing the higher-order errors. The determination of the reference state of atoms, used for pseudopotential construction—that should be chosen as close as possible to the environment where the pseudopotential will be used in order to reduce all kinds of errors—relies on an intuitive choice within the standard pseudopotential-construction techniques, contrary to the technique presented here.

Let us examine the reduction of error by the AEPP approach from the viewpoint of the preceding considerations. By definition, the reference state of the atom used for pseudopotential generation is chosen in the ''center of mass'' of the electronic bands in the solid, corresponding to the atomic valence wave functions. By that, the optimum position for the pseudopotential energy windows is achieved. In addition, the frozen-core approximation is avoided, i.e., the core states are relaxed and recalculated consistently in the solid, which represents an additional degree of optimization for the reference state.

The higher-order errors in the energy transferability can be significantly reduced by using pseudofunctions with a node, as shown in Figs. 2 and 3 below. By optimizing the reference energy for the semicore state, the energy window extends. Satisfying the norm-conserving condition even for the semicore states results in a very transferable pseudopotential over a wide energy window but it sometimes causes a reduction in the effective cutoff radius and leads to hard pseudopotentials. A transferable and efficient pseudopotential can be obtained by including the semicore norm-conserving condition among less strictly weighed optimization conditions balanced with ''smoothness'' conditions.

The first-order transferability error in the exchange and correlation potential terms can be avoided, such as in the standard pseudopotential method, by the NLCC, where the relaxed self-consistent core charge density can be used [this approach could be denoted as a self-consistent NLCC (SCNLCC)]. As a reasonable representation for the core charge density we successfully tested the short expansion (three terms) of Gaussian orbitals with optimized α parameters, which implies suitable pseudization of the core charge and ensures a sufficiently accurate description in the region relevant with respect to the chemical bonds.

In fact, however, it should be noted that for the all-electron pseudopotential optimized and used for a given structure, the NLCC (or SCNLCC) has no meaning since exactly the same charge density is used for unscreening and rescreening the pseudopotential. The need for the NLCC/SCNLCC arises only on condition that the same pseudopotential—without additional relaxation—is used for varying atomic positions (and, consequently, for varying charge distribution), e.g., for molecular-dynamics calculations, which is more demanding with respect to the pseudopotential transferability.

Even if the NLCC is not used, the AEPP method gives good results for structure parameters as a consequence of the optimum choice of reference state for pseudopotential construction. By that, the transferability becomes much less important for most applications than in the case of standard, free-atom-based pseudopotentials. This fact can be used—in those cases when no significant changes of atomic positions are supposed—for constructing less transferable, extremely soft pseudopotentials.

It should be noted that the AEPP is intended to be generated specifically for a particular external environment, i.e., for a particular structure and types of neighboring atoms. Therefore, the transferability of AEPP from one solid to another has not been discussed explicitly so far nor does the next section contain test calculations of this kind. In the rest

of this section we append several notes concerning this question.

In Ref. 3, we examined the extent to which a particular AEPP is correct for various configurations of an isolated (free) atom in vacuum, which we use as an example of a significantly different environment. We suppose, according to our experience, that a vacuum is more of a different environment compared to a solid than is the common difference between two solids containing a particular type of atom. Accordingly, using AEPP for the calculation of free pseudoatoms having different atomic configurations, with asymptotically vanishing pseudofunctions (contrary to any valence wave function in a solid or molecule), is a very stringent test of this kind of transferability. The eigenvalues and eigenvectors are compared with the all-electron calculations of a free atom with the same configuration. This way, the standard transferability of atomic-based pseudopotentials from an atom (using an *ad hoc* ''suitable atomic configuration'') to a solid is reversed. This test was performed even for a pair of AEPP's of a particular element derived from different structures (e.g., Ti in TiC and TiS_2, Si in $CoSi_2$ and Si crystals etc.) with very satisfactory results.

In fact, this kind of pseudopotential transferability (i.e., from one structure to another), in principle, does not differ from the transferability of type (ii) mentioned above (i.e., with respect to varying the external charge density). Above we have described the features of the AEPP that allow substantial improvement also in this kind of transferability, particularly by means of the pseudofunction with a node, compared to standard pseudopotentials.

Summing up, in the case of the AEPP derived for one solid and transferred to another solid, the advantage of an optimum reference state of the AEPP is partially lost, but still—since the common difference between solids is much smaller than the difference between a solid and vacuum and since the AEPP can be constructed with higher transferability of type (ii) than standard pseudopotentials—significantly higher precision is achieved than with standard pseudopotential techniques in common cases. If such aim is taken into account in the pseudopotential-generating process (e.g., for molecular-dynamics calculations), excellent transferability can be reached compared to standard similarly ''soft'' (or ''hard'') one-energy-channel pseudopotentials derived from the ground-state configuration of a free atom.

IV. EXAMPLES OF APPLICATIONS

In this section we show the application and results of the presented approach for some examples of materials where conventional pseudopotential techniques meet serious difficulties. In all subsequent calculations the exchange-correlation functional used was that of Ceperley and Alder[11] as parametrized by Perdew and Zunger.[12] Calculations were made using the AEPP in a plane-wave basis.

A. Structural properties of graphite

The extensive discussion of the important factors for the representation of cohesion between graphitic structures was presented quite recently by Girifalco and Hodak.[13] Their analysis shows that first-principles calculations for graphitic structures can be carried out quite successfully, but they are sensitive to the details of calculation. Particularly, DFT-local-density approximation (LDA) calculations are sensitive to the choice of pseudopotential, the basis set, and the number of basis functions used in the wave-function expansion. In a rich list of references, the authors of Ref. 13 document failures and spurious results of various calculations, notably for the calculations of the interplanar binding energy.

TABLE I. Comparison of theory and experiment for the zero-presure lattice parameters a_0 and c_0 (a.u.) of graphite in the Bernal structure. Full potential linearized augmented plane wave is denoted as FLAPW and the linear combination of Gaussian orbitals as LCGO.

Source	Reference	a_0 (a.u.)	c_0 (a.u.)
Pseudopotential	25	4.667	13.323
Pseudopotential	15	4.632	12.661
Pseudopotential	26	4.611	12.622
FLAPW	27	4.647	12.903
LCGO	28	4.626	12.819
This work		4.628	12.784
Experiment (0 K)	29	4.652	12.780
(293 K)	30	4.651	12.678

We studied hexagonal $ABAB\cdots$ stacked graphite (Bernal structure) having several (two to four) layers in a unit cell. We minimized the total energy with respect to a and c lattice parameters, obtaining values of $a=2.449$ Å and $c=6.765$ Å. Cutting out one layer we created a gap of double interlayer distance. To be sure that this distance is sufficient to prevent any interaction we tested using an even wider gap.

The self-consistent charge and potential were determined using both six and twelve special k points[14] in the irreducible Brillouin zone (IBZ). As in the work of Schabel and Martins,[15] good convergence of the calculated properties with respect to the number of k points was found. The energy cutoff for the plane-wave expansion was tested for $E_{\mathrm{cut}}=40$, 48, and 56 Ry; the 48 Ry yielded stable and convergent results. Our results are compared with the other calculations in Table I.

The interplanar binding energy, which is the difference between the bulk and monolayer total energy, was calculated in a following way: At first we calculated the total energy of the graphite E_{gr} represented by four atoms (two layers) in a hexagonal unit cell. Then we removed one layer from this unit cell and repeated the calculation; the same program, pseudopotential, basis, etc. were used in both cases. In order to be sure that the interaction of monolayers in the supercell did not affect the results in a significant way, we performed the same calculations for the supercell structures with larger c lattice parameter. The resulting interplanar energies for various supercells lie in an interval $E_i=(0.02-0.03$ eV) which is in very good agreement with the best all-electron calculations up to date. The wide range of calculated E_i in Table II values is indicative of the extreme sensitivity of the predicted interplanar binding energy to computational details and theoretical assumptions. Some caution with regard to the

TABLE II. Interplanar binding energies E_i (in eV/at.) in various graphite structures.

System	Reference	$-E_i$(eV/at.)
The *AB* two layer	31	0.03
	32	0.15
The *ABAB* . . . crystal	27	0.10–0.06
	33	0.06
	15	0.024
This work		0.03–0.02
Experiment	34	0.03–0.02

close agreement with experiment may be advisable, however, in view of the (i) well-known strong temperature dependence of graphite lattice dynamics and (ii) sensitivity of the experimental value to the presence of stacking faults, defects, and impurities.

B. Gallium "3*d* problem" in GaN

Gallium 3*d* electrons are a nice example of semicore states. Since the great potential for technological applications was discovered, GaN has been addressed by a number of theoretical investigations. The performance of various pseudopotentials treating the Ga 3*d* states with different techniques is given, e.g., in Refs. 16 and 17. First, the gallium 3*d* electrons were included in the core of the Ga atom. The frozen core with 3*d* electrons then depends on the construction of the pseudopotential. Secondly, the effect of gallium 3*d* orbitals was taken into account directly by assuming that the 3*d* electrons were part of the valence states. In both cases, the NLCC (using the charge density of all the states considered to be core states) can be applied. It is evident that in the first case (3*d* in a core) the NLCC is more important. Recently, the problem of the construction of accurate pseudopotentials in the case of GaN (and also AlN and InN) was analyzed in Ref. 18.

Another alternative to include the semicore 3*d* electrons is to use self-interaction-corrected (SIC) and self-interaction- and relaxation-corrected pseudopotentials.[19] The all-electron calculations can serve as a test of approximations employed.

We applied the AEPP technique in the simplest way, i.e., with the relaxed core containing the relaxed Ga 3d electrons. In this way we needed no more than three iteration loops for the self-consistency of the AEPP. A kinetic-energy cutoff $E_{cut}=60$ Ry was satisfactory, and ten special *k* points in the IBZ were used. Our results in comparison with the results of other techniques are given in Table III. We see that including the 3*d* electrons into the frozen core results in quite disperse values of lattice constants and bulk moduli of GaN. Evidently, the results depend on the construction of the core region of a Ga pseudopotential via "technical parameters" (cutoff radii, atomic configuration). On the other hand, the results when treating the *d* states as valence states are much more stable, of course at the expense of harder pseudopotentials and higher E_{cut} at about 80 Ry.[16] The all-electron results are very similar to each other and in very good agreement, as expected, with the AEPP values.

TABLE III. Calculated lattice constants a_0 (Å), bulk moduli B_0 (GPa), and derivatives B' of bulk zinc-blende GaN. All the results are based on LDA, and all the pseudopotential calculations use the plane-wave basis set. Pseudopotential is denoted as PP, CASTEP is a computer code, and full potential linear muffin-tin orbital is FPLMTO.

Method	Reference	a_0	B_0	B'
PP, 3*d* frozen in core	35	4.47	1.79	3.93
	36	4.30	2.40	
	37	4.42	1.73	
	17	4.33	2.38	
	38	4.30	2.51	2.76
-NLCC	17	4.44	1.93	
PP, 3*d* valence	39	4.460	1.87	
	40	4.524	2.06	3.7
	41	4.519	2.00	4.15
	16	4.518	1.91	4.14
	17	4.48	2.18	
-Ultrasoft CASTEP	42	4.46	1.99	
SIC PP, 3*d* valence	19	4.56		
FPLMTO	43	4.46	2.01	3.9
	44	4.466	1.98	
FLAPW	45	4.488	2.06	4.6
This work		4.504	2.03	4.4
Experiment	46	4.50	1.90	

C. Transition-metal carbides and nitrides

Quite another problem for the standard pseudopotential technique arises in the transition metal (TM) element–carbon or the TM–nitrogen bonds. At this point we do not mean the "standard" difficulty with 3*d* or 4*d* states of TM elements: The hidden problem is related to the last nodes of valence wave functions of TM elements.

In our recent work[20] we studied ground-state properties of TM carbides and nitrides. Very good agreement was observed between our calculations and other results obtained by a standard pseudopotential technique,[21] but both pseudopotential techniques yield noticeably smaller bulk moduli than the all-electron full potential linearized augmented plane-wave (FLAPW) technique.[22,23] The reason for the disagreement has been found (see Ref. 20) in the insufficient description of valence electrons by nodeless pseudofunctions. Constructing valence *s* and *p* pseudofunctions of TM elements with a node, we obtained bulk moduli very close to the FLAPW results, as shown in Table IV.

The reason the nodeless pseudofunctions do not accurately describe valence wave functions follows from the fact that the most distant nodes of the valence *s* and *p* functions of TM elements are too apart with respect to the very short interatomic distances in TM carbides and nitrides. The nodeless pseudofunction, contrary to the pseudofunction having a node corresponding to the most distant node of the true valence function, cannot describe the crystal charge density in the bond region correctly (see Fig. 1). As a consequence, in this region the pseudocharge density is "smoother" and the bulk modulus is smaller.

TABLE IV. Calculated lattice constants and bulk moduli of a series of TM carbides and nitrides. AEPP-I and AEPP-II denote the all-electron pseudopotentials with pseudowave functions without node and with one node, respectively. Abbreviations CA and HL in parentheses following the names of the methods denote using the exchange and correlation potentials of Refs. 11 and 47, respectively.

Method		PP(CA)		AEPP-I(CA)		FLAPW(HL)		AEPP-II(CA)	
	a_{exp} (a.u.)	a_0/a_{exp} (%)	B_0 (GPa)	a_0/a_{exp} (%)	B_0 (GPa)	a_0/a_{exp} (%)	B_0 (GPa)	a_0/a_{exp} (%)	B_0 (GPa)
ZrC	4.683			98.7	233			98.8	253
TiC	4.319	101.4[a]	267[a]	98.0	277	99.9[c]	286[c]	98.6	303
NbC	4.469			99.3	305			99.3	332
VC	4.182	100.9[a]	321[a]	98.0	326	98.9[c]	348[c]	98.0	356
ZrN	4.610			98.6	251	98.3[d]	292[d]	98.2	290
TiN	4.235	98.6[b],102.0[a]	319[b],304[a]	98.2	310	101.5[c],98.7[d]	326[c],322[d]	99.0	331
NbN	4.392			99.0	321	99.3[d]	353[d]	99.6	361
VN	4.128	101.5[a]	338[a]	98.3	338	99.1[c],98.4[d]	370[c],376[d]	98.6	383

[a]Troullier and Martins pseudopotential, Ref. 21.
[b]Ultrasoft pseudopotentials, Ref. 48.
[c]FLAPW, Ref. 23.
[d]FLAPW, Ref. 22.

A side effect of using the pseudowave function with a node is the existence of another, deeper, electronic state, corresponding to the nodeless pseudowave function. By optimizing the pseudopotential, this state can be tuned so as to correspond to a real semicore state, or it can be kept unoccupied. From a technical point of view the state corresponding to the nodeless pseudofunctions can be easily distinguished in the band structure and does not cause a computational problem. The only condition to be satisfied is a consistent unscreening and rescreening of the potential in both the pseudopotential-generating process and in using the pseudopotential in a solid.

D. Alkali chlorides

In this subsection we describe using the AEPP technique for NaCl and other chlorides and show the variability of this technique. There are several reasons why we have chosen the series of alkali chlorides. (i) There is significant disagreement between results of ground properties of NaCl (lattice constant and bulk modulus) obtained by various first-principles techniques. (ii) In view of the relatively easily polarizable valence shell of first-column elements (Li, Na, K, and Rb), their core-valence overlap in chlorides departs considerably from the free atom; according to Porezag *et al.*,[4] applying the NLCC is an absolute necessity for alkali atoms. Therefore we consider chlorides to be a particularly difficult case for pseudopotential methods (with regard to the transferability) that is suitable for demonstrating AEPP properties even without the NLCC.

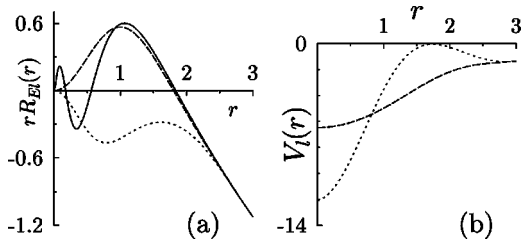

FIG. 1. Radial *p*-wave functions of Zr in ZrC: all-electron $5p$ function (solid line), single node pseudofunction (dashed line), nodeless pseudofunction (dotted line) (a), and corresponding pseudopotentials (b). Atomic units are used for both axes.

The AEPP method makes possible several different ways to treat semicore states of alkali atoms. For better understanding we display the possibilities in the case of the Na atom graphically.

In Fig. 2, the pseudowave functions for both the valence and the semicore states and corresponding pseudopotentials of Na in NaCl are shown for several cases: in the case of norm-conserving pseudopotentials for both energy windows (first row), for non-norm-conserving relaxed pseudopotentials for the semicore states (second row), and for unoccupied semicore states (third row). The difference between the smooth ''semi-norm-conserving'' pseudopotential and the fully norm-conserving pseudopotential approaching the all-electron potential at an effectively reduced cutoff radius (as a result of the norm-conserving condition) is evident.

For comparison, we present also the one-energy-window pseudopotentials generated by the all-electron pseudopotential scheme from the charge density obtained by the previous two-energy-window calculation (fourth row). These pseudopotentials give correct results (even without any NLCC) and they are very soft, but, since their transferability is extremely narrow, the only way to obtain them is via other more transferable pseudopotentials.

In Fig. 3 the energy transferability in terms of logarithmic derivatives is shown. For comparison, the curves corresponding to the example of a free-atom-based pseudopotential are given, too. The displayed pseudopotentials have very different properties in several respects, e.g., their behavior in Fourier space significantly differs: Figure 4 demonstrates the plane-wave convergence for various types of pseudopotentials.

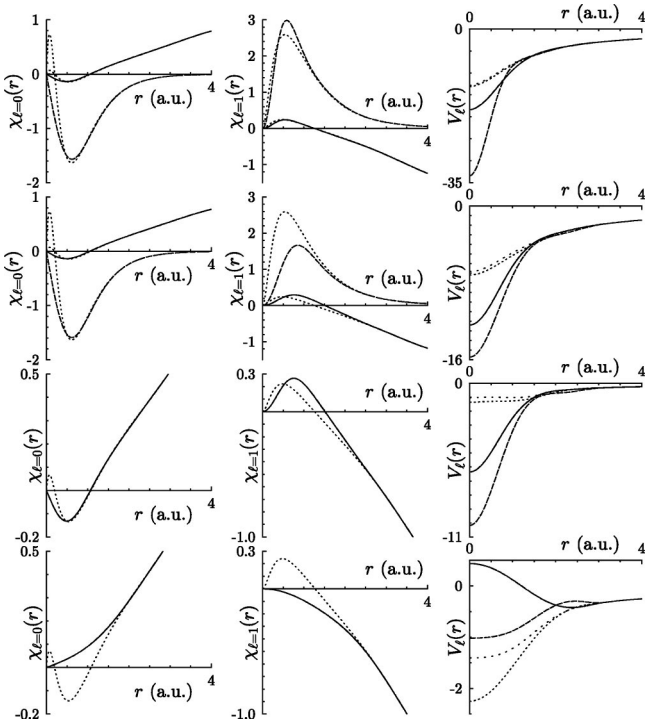

FIG. 2. Radial wave functions and corresponding unscreened pseudopotentials generated by the AEPP scheme for Na in NaCl in four cases: norm-conserving semicore states (first row), non-norm-conserving semicore states (second row), non-norm-conserving unoccupied semicore states (third row), and no semicore states (fourth row). In the first and second columns (s and p pseudowave functions, respectively), the solid and dashed lines correspond to the valence and semicore pseudowave functions. The dotted curve approaching the solid or dashed curve represents the corresponding all-electron wave function for each case. The wave functions have been multiplied by r and normalized so that they (squared) form the correct crystal charge density. In the third column, the solid, dashed, densely dotted, and sparsely dotted lines correspond to s, p, d, and f unscreened pseudopotentials, respectively. Notice the vertical energy scale (atomic units) in the third column.

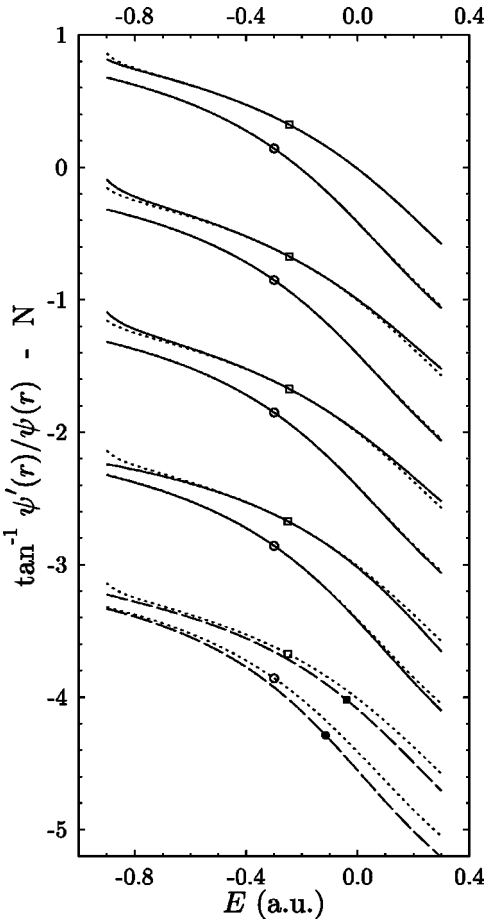

FIG. 3. Logarithmic derivatives for s and p radial valence wave functions of Na in NaCl for four types of AEPP's, in the same order as in Fig. 2 (solid lines). The curves have been shifted by $-N$ (0,1,2,3) according to the order of pseudopotentials. The reference energies are marked by circles (s potentials) and squares (p potentials). The dotted lines correspond to the all-electron potential provided by the AEPP procedure. The lowest curves (dashed lines), shifted by -4, show the logarithmic derivatives related to the neutral free atom in the configuration $3s^{0.8}3p^{0.1}3d^{0.1}$ (the configuration used in Ref. 10), compared to the all-electron AEPP curves (dotted lines). The filled circle and square mark the atomic eigenvalues that are usually used as reference energies in generating standard pseudopotentials.

All four pseudopotentials presented above yield the same results for the case of NaCl. Table V summarizes the calculated primary structure parameters for all the alkali chlorides under study.

Finally, we notice the valence charge distribution in these compounds and its consequences for the construction of the AEPP. Table VI shows the valence radial partial charges around atoms in crystals of NaCl and KCl for various sphere radii. It should be noted at this point that we do not deal with the question of whether the p, d, and f electrons related to the Na (or K) atomic sites really ''belong'' to these atoms (irrespective of any physical meaning of these words) or if the charges listed in the table are just caused by the mathematical effect of the projection operator upon the crystal wave functions. In any case, the pseudopotential should act on these components of the crystal charge density correctly, simulating the effect of the all-electron potential under the given conditions. Consequently, considering the construction of nonlocal pseudopotentials for Na and K, even the f component of the pseudopotential should not be neglected since the f electrons form about 8% of the total charge inside the sphere centered on Na (in the case of Na in NaCl) where the pseudopotential is angular dependent (see Fig. 2). On the other hand, for Cl in KCl, the d pseudopotential and higher l components have no meaning since there is almost no charge corresponding to these projections.

V. SUMMARY

In this paper we discuss various aspects of pseudopotential transferability and introduce ways of improving accuracy and transferability in several respects, demonstrated on a series of compounds. The approaches to improving accuracy are considered for (i) extending the transferability range in

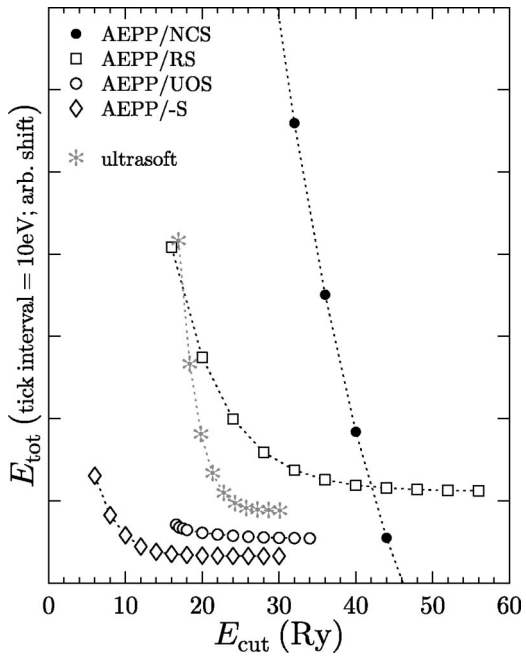

FIG. 4. Plane-wave cutoff convergence for four types of AEPP's, in the same order as in Fig. 2: (i) with norm-conserving semicore states (NCS), (ii) relaxed semicore states (RS), (iii) unoccupied semicore states (UOS), and (iv) with no semicore states/nodeless valence pseudowave functions (-S). For comparison, the convergence with an ultrasoft (Ref. 7) pseudopotential calculated with the CASTEP computer code is depicted (Ref. 50).

various aspects (transferability with respect to scattering properties, external charge density, unscreening/rescreening process) and (ii) an optimum choice of pseudopotential-constructing reference state, implying an optimum position of the transferability range.

We demonstrate the adaptability and accuracy of the all-electron pseudopotential technique where the transferability range is located optimally with respect to the charge distribution in the solid. In addition, we illustrate using the noded pseudowave function for extending the transferability. With that, a more accurate charge distribution is obtained and, consequently, all kinds of transferability are improved. We show that in some cases the noded pseudowave function implicates even an softer pseudopotential reducing the necessary basis set size. In this case, the charge of the semicore states can replace the approximated core charge of the nonlinear core correction (NLCC) used to reduce the exchange-correlation potential term errors in other pseudopotential techniques. Even in the case of unoccupied semicore states and no NLCC we get correct results for structural parameters of chlorides, which confirms the essential role of positioning the transferability range properly.

The accuracy of DFT is ultimately governed by the quality of the exchange-correlation (XC) functional and how well it approximates the nonlocal nature of XC interactions. A great deal of understanding has been gained from the LDA and intensive research for more sophisticated XC functionals is under way (see, e.g., Ref. 24 and references therein). However, the accuracy of the XC approximation can be verified only by computational techniques fulfilling the precision beyond the differences in XC functionals themselves. The purpose of this paper is to demonstrate (i) that in some cases the precision of the standard computational techniques is not satisfactory from this point of view, and (ii) how this high precision can be achieved.

TABLE V. Lattice constants (Å) and bulk moduli (GPa) calculated with the AEPP's.

	a_0	a_{exp}	B_0	B_{0exp}
LiCl	4.92	5.08[a]	39.2	33.4[a]
NaCl	5.48	5.64[a]	33.1	26.6[a]
KCl	6.16	6.29[a]	19.2	19.7[a]
RbCl	6.34	6.58[a]	21.3	19.5[a]

[a]Reference 49.

TABLE VI. Partial *l*-projected charges (integrated radial charge densities) for atoms in NaCl and KCl, for several radii approaching the ''valence'' radius, i.e., the radius of the sphere containing the same amount of valence charge as a free neutral atom. The radius *r* is in atomic units. In the second column, the total charge in the sphere of radius *r* is given. *l*-projected partial charges for $l=0,1,2,3$ are in remaining columns.

	r	Total	*s*	*p*	*d*	*f*
Na	2.4	0.241 26	0.077 11	0.107 02	0.044 79	0.009 24
(NaCl)	2.6	0.356 35	0.108 86	0.148 85	0.073 64	0.018 35
	2.8	0.526 52	0.149 08	0.210 24	0.117 63	0.034 90
	3.0	0.773 82	0.198 92	0.295 99	0.183 36	0.063 76
	3.2	1.128 65	0.259 66	0.411 30	0.279 17	0.112 29
Cl	2.2	5.673 24	1.682 49	3.985 88	0.003 91	0.000 24
(NaCl)	2.4	6.168 41	1.778 76	4.382 81	0.005 64	0.000 47
	2.6	6.570 16	1.847 78	4.712 74	0.008 10	0.000 75
	2.8	6.894 11	1.896 69	4.983 73	0.011 45	0.001 28
	3.0	7.155 63	1.931 47	5.204 41	0.016 04	0.002 30
K	2.8	0.513 59	0.046 46	0.367 05	0.084 87	0.015 21
(KCl)	3.0	0.604 17	0.065 07	0.398 78	0.108 79	0.031 53
	3.2	0.733 64	0.089 53	0.439 30	0.149 56	0.055 25
	3.4	0.918 78	0.120 96	0.494 58	0.205 81	0.097 43
	3.6	1.182 67	0.160 58	0.569 21	0.283 42	0.169 46
Cl	2.4	5.847 57	1.502 21	4.340 99	0.003 82	0.000 03
(KCl)	2.6	6.237 88	1.566 07	4.669 15	0.002 99	0.000 33
	2.8	6.550 68	1.613 13	4.931 98	0.005 54	0.000 55
	3.0	6.800 47	1.648 04	5.147 97	0.001 06	0.003 40
	3.2	7.001 11	1.674 51	5.319 37	0.002 93	0.004 30

ACKNOWLEDGMENT

This work was supported by the Grant Agency of the Academy of Sciences of the Czech Republic, Grant Nos. A1010317, A101906, and 202/02/0841/A. The authors are also grateful for the financial assistance provided by NATO Grant No. PST.CLG.979025.

[1] W. E. Pickett, Comput. Phys. Rep. **9**, 115 (1989).
[2] M. C. Payne, M. P. Teter, D. C. Allan, T. A. Arias, and J. D. Joannopoulos, Rev. Mod. Phys. **64**, 1045 (1992).
[3] J. Vackář, M. Hyt'ha, and A. Šimůnek, Phys. Rev. B **58**, 12712 (1998).
[4] D. Porezag, M. R. Pederson, and A. Y. Lin, Phys. Rev. B **60**, 14132 (1999).
[5] J. Vackář and A. Šimůnek, Solid State Commun. **81**, 837 (1992).
[6] D. R. Hamann, Phys. Rev. Lett. **43**, 1494 (1979); Phys. Rev. B **40**, 2980 (1989).
[7] D. Vanderbilt, Phys. Rev. B **41**, 7892 (1990).
[8] W. C. Topp and J. J. Hopfield, Phys. Rev. B **7**, 1295 (1973).
[9] E. L. Shirley, D. C. Allan, R. M. Martin, and J. D. Joannopoulos, Phys. Rev. B **40**, 3652 (1989).
[10] S. G. Louie, S. Froyen, and M. L. Cohen, Phys. Rev. B **26**, 1738 (1982).
[11] D. M. Ceperley and B. J. Alder, Phys. Rev. Lett. **45**, 566 (1980).
[12] J. F. Perdew and A. Zunger, Phys. Rev. B **23**, 5048 (1981).
[13] L. A. Girifalco and M. Hodak, Phys. Rev. B **65**, 125404 (2002).
[14] D. J. Chadi and M. L. Cohen, Phys. Rev. B **8**, 5747 (1973).
[15] M. C. Schabel and J. L. Martins, Phys. Rev. B **46**, 7185 (1992).
[16] C. Stampfl and C. G. Van de Walle, Phys. Rev. B **59**, 5521 (1999).
[17] R. Miotto, G. P. Srivastava, and A. C. Ferraz, Phys. Rev. B **59**, 3008 (1999).
[18] M. Fuchs, J. L. F. Da Silva, C. Stampfl, J. Neugebauer, and M. Scheffler, Phys. Rev. B **65**, 245212 (2002).
[19] D. Vogel, P. Krueger, and J. Pollmann, Phys. Rev. B **55**, 12836 (1997).
[20] A. Šimůnek and J. Vackář, Phys. Rev. B **64**, 235115 (2001).
[21] J. C. Grossmann, A. Mizel, M. Côté, M. L. Cohen, and S. G. Louie, Phys. Rev. B **60**, 6343 (1999).
[22] C. Stampfl, W. Mannstadt, R. Asahi, and A. J. Freeman, Phys. Rev. B **63**, 155106 (2001).
[23] W. Wolf, R. Podloucky, T. Antretter, and F. D. Fischer, Philos. Mag. B **79**, 839 (1999).
[24] P. R. Rushton, D. J. Tozer, and S. J. Clark, Phys. Rev. B **65**, 193106 (2002); M. Fuchs and X. Gonze, *ibid.* **65**, 235109 (2002).
[25] M. T. Yin and M. L. Cohen, Phys. Rev. B **29**, 6996 (1984).
[26] J. Furthmüller, J. Haffner, and G. Kresse, Phys. Rev. B **50**, 15606 (1994).
[27] H. J. F. Jansen and A. J. Freeman, Phys. Rev. B **35**, 8207 (1987).
[28] J. C. Boettger, Phys. Rev. B **55**, 11202 (1997).
[29] Von A. Ludsteek, Acta Crystallogr., Sect. A: Cryst. Phys., Diffr., Theor. Gen. Crystallogr. **28**, 59 (1972).
[30] J. Donohue, *The Structures of the Elements* (Krieger, Malabar, FL, 1982), p. 256.
[31] S. B. Trickey, F. Müller-Plathe, G. H. F. Diercksen, and J. C. Boettger, Phys. Rev. B **45**, 4460 (1992).
[32] S. B. Trickey, G. H. F. Diercksen, and F. Müller-Plathe, Astrophys. J. Lett. **336**, L37 (1989).
[33] R. H. Bauhgman, H. Eckhardt, and M. Kertesz, J. Chem. Phys. **87**, 6687 (1987).
[34] L. A. Girifalco and R. A. Lad, J. Chem. Phys. **25**, 693 (1956).
[35] A. Munoz and K. Kunc, Phys. Rev. B **44**, 10372 (1991).
[36] B. J. Min, C. T. Chan, and K. M. Ho, Phys. Rev. B **45**, 1159 (1992).
[37] P. E. Van Camp, V. E. Van Doren, and J. T. Devreese, Solid State Commun. **81**, 23 (1992).
[38] S. J. Jenkins, G. P. Srivastava, and J. C. Inkson, J. Phys.: Condens. Matter **6**, 8781 (1994).
[39] A. F. Wright and J. S. Nelson, Phys. Rev. B **51**, 7866 (1995).
[40] V. Fiorentini, A. Satta, D. Vanderbilt, S. Massida, and F. Meloni, in *The Physics of Semiconductors*, edited by D. J. Lockwood (World Scientific, Singapore, 1995), p. 137.
[41] A. Satta, V. Fiorentini, A. Bosin, and F. Meloni, in *Gallium Nitride and Related Materials*, edited by R. D. Dupuis, J. A. Edmond, F. A. Ponce, and S. Nakamura, Mater. Res. Soc. Symp. Proc. 395 (MRS, Pittsburgh, 1966), p. 515.
[42] P. P. Rushton, S. J. Clark, and D. J. Tozer, Phys. Rev. B **63**, 115206 (2001).
[43] K. Kim, W. R. Lambrecht, and B. Segall, Phys. Rev. B **53**, 16310 (1996).
[44] V. Fiorentini, M. Methfessel, and M. Scheffler, Phys. Rev. B **47**, 13353 (1993).
[45] Su-Huai Wei and A. Zunger, Phys. Rev. B **60**, 5404 (1999).
[46] *Properties of Group-III Nitrides*, edited by J. H. Edgar, EMIS, Datareview Series (IEE, London, 1994).
[47] L. Hedin and B. I. Lundqvist, J. Phys. C **4**, 2064 (1971).
[48] M. Marlo and V. Milman, Phys. Rev. B **62**, 2899 (2000).
[49] J. R. Hardy and A. M. Karo, *The Lattice Dynamics and Statics of Alkali Halide Crystals* (Plenum, New York, 1979).
[50] M. Hyt'ha (unpublished).